Check for updates

# Designing solution chemistries for the low-temperature synthesis of sulfide-based solid electrolytes†

Hee-Dae Lim, Xiujun Yue, Xing Xing, Victoria Petrova, Matthew Gonzalez, Haodong Liu and Ping Liu ⓘ *

Developing synthesis methods for high quality solid electrolytes has been a key issue for enabling all-solid-state batteries. As compared to conventional methods using mechanical ball milling, liquid-phase synthesis methods would provide a facile way to produce solid electrolytes by reducing the reaction time and heating temperature. The simplified process is also potentially applicable to scalable manufacturing. Here, we introduce a new solution-based synthesis method for an $Li_2S$–$P_2S_5$ solid electrolyte by adding a nucleophilic agent, $LiSC_2H_5$. The strong nucleophile can break the P–S bonds of $P_2S_5$, fully dissolving the $P_2S_5$ in tetrahydrofuran (THF) and forming soluble intermediates. The modified synthesis protocol provides kinetically favorable conditions for $P_2S_5$ to react with the insoluble $Li_2S$, demonstrating the formation of a high quality β-$Li_3PS_4$ solid electrolyte ($1.32 \times 10^{-4}$ S cm$^{-1}$) with a uniform particle shape.

Solid electrolytes (SEs) have been a key element to solving the prevailing safety issues of current lithium ion batteries using flammable organic electrolytes.[1–4] Among many candidates, sulfide-based SEs have attracted enormous attention due to their high conductivities.[4–6] However, conventional synthesis methods for sulfide-based SEs are energy-intensive, require high temperature and pressure conditions and take a long time to produce a final product. For example, $Li_2S$–$P_2S_5$ (*i.e.*, LPS) SEs have been mechanically synthesized by using high-energy ball milling followed by repeated sintering and pressurizing steps.[7–9]

Alternatively, liquid-phase synthesis (or solution-based synthesis) methods have been developed, providing a much faster and simpler way of synthesizing sulfide-based SEs compared to conventional methods.[10–12] The solvent medium helps to promote a reaction between $Li_2S$ and $P_2S_5$ and provides enough energy to form final products such as $Li_3PS_4$ and $Li_7P_3S_{11}$, which greatly reduces both the sintering temperature

*Department of Nanoengineering, University of California, La Jolla, San Diego, CA 92093, USA. E-mail: piliu@eng.ucsd.edu*

and synthesis time. Various solvents such as THF,[11,12] acetonitrile (ACN),[12–14] dimethyl carbonate (DMC),[15] and 1,2-dimethoxyethane (DME)[16] have been utilized for synthesizing LPS SEs. Normally, the insoluble precursors of $L_2S$ and $P_2S_5$ are dispersed in a solvent and stirred for a few days to react with each other. Then, the solution is filtered to collect a powder, which is compressed into an SE pellet. However, due to the insolubilities of precursors, unwanted residuals or by-products might precipitate together with the final product during the filtering or drying process.[10,14] In addition, the solution itself has rarely been applied as a direct coating on anode and cathode materials due to the precipitated particles. Although solvents with high dielectric constants (DCs) such as *N*-methylformamide (NMF),[17–19] and hydrazine[20] have succeeded in dissolving precursors or final products (*e.g.*, $Li_3PS_4$ and $Li_3P_7S_{11}$), their application is still limited due to the high reactivity of solvents, which can vigorously react with the Li metal and cell components.

Here, we developed a new synthesis route for sulfide-based SEs by using a nucleophilic agent, $LiSC_2H_5$ (lithium thioethoxide, LiSEt). It is first demonstrated that a chemical reaction between LiSEt and $P_2S_5$ forms the intermediate soluble compounds of LiSEt·$P_2S_5$ in a moderate DC solvent of THF. The dissolved $P_2S_5$ composite can then further react with $Li_2S$ (s) resulting in the formation of a conductive β-$Li_3PS_4$ SE. This modified method can produce a homogenous and purified β-$Li_3PS_4$ SE since soluble residuals or by-products can be completely removed during filtration. In addition, it provides kinetically favorable conditions (the reaction between two reactants of liquid and solid phases), which cannot be achieved by following conventional methods.

Our strategy to synthesize SEs is to make a soluble intermediate reactant in THF in order to drive a reaction between liquid and solid phase reactants, rather than using the conventional solid-to-solid phase reaction. For a better understanding of the difference between the modified solution-based synthesis method and previous methods, a schematic illustration is provided in the ESI (Fig. S1†). We used LiSEt as an
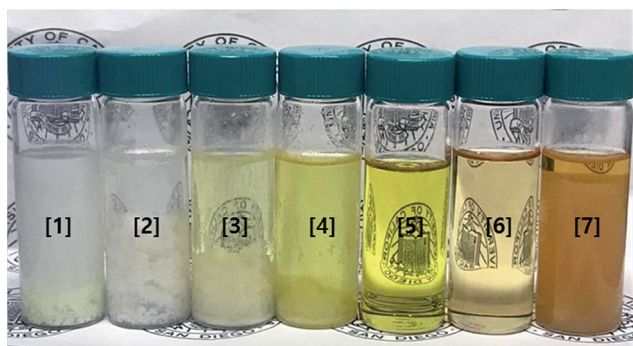
Fig. 1 Images of THF solutions dissolving $P_2S_5$ and $LiSC_2H_5$ with different molar ratios of 1 : 0, 1 : 0.1, 1 : 0.3, 1 : 0.5, 1 : 1, 1 : 3, and 1 : 6 from [1] to [7], respectively. 10 g of THF solvent is used in each solution.

additive to make $P_2S_5$ soluble in THF because its strong nucleophilicity[21,22] is expected to break P–S bonds in $P_2S_5$. To test the effect of LiSEt on the solubility of $P_2S_5$, LiSEt with different molar ratios was mixed with $P_2S_5$ as shown in Fig. 1. Reference solution [1] (only $P_2S_5$ without $LiSC_2H_5$) precipitated most of the $P_2S_5$ as powders even after stirring for one day. As LiSEt was added to a solution, precipitates decreased as observed in solutions [1] to [4]. It should be noted that solution [5] (*i.e.*, 1 : 1 ratio of $P_2S_5$ and LiSEt) is transparent, suggesting that $P_2S_5$ can fully react with LiSEt and form certain soluble compounds. Although the solutions with high ratios of LiSEt ([6] and [7] with ratios of 1 : 3 and 1 : 6, respectively) can also dissolve $P_2S_5$, focus is placed on solution [5] because it can fully dissolve $P_2S_5$ with a minimal amount of LiSEt.

Nuclear magnetic resonance (P-NMR), Fourier transform-infrared spectroscopy (FT-IR), and Raman spectroscopy were utilized to analyze solution [5] (Fig. 2). While the pristine $P_2S_5$ shows a sharp single characteristic peak at 57.3 ppm,[23] it is not dominant in solution [5]; instead, a small and broad bump is observed in the spectrum of solution state $P^{31}$ NMR (Fig. 2a). It is also noted that new peaks at 118 and 88 ppm, which are attributed to $P(SR)_3$ and $PS_4^{3-}$, respectively,[24–26] are detected,

implying that P–S bonds in the pristine $P_2S_5$ are broken. Many of the new peaks between 110 and 90 ppm, which are also undetectable in the pristine $P_2S_5$, demonstrate the formation of various phosphorous bonding features in the solution. Phosphorous bonds with sulfur species are either ionic with a negative charge (as in $PS_4^{3-}$) or covalently bonded to carbon (as in a P–S–Et configuration). It is reasonable to attribute the peaks between 110 and 90 ppm to thiophosphate species with a mixture of ionic and covalently bonded sulfur atoms. Additional results from NMR experiments on changing the molar ratio between LiSEt and $P_2S_5$ are provided in Fig. S2.† Therefore, it is concluded that the addition of LiSEt can trigger the bond breaking of $P_2S_5$ resulting in the formation of soluble composites (*i.e.*, $LiSEt \cdot P_2S_5$) with various phosphor bonding features.

To further elucidate the reaction between LiSEt and $P_2S_5$, FT-IR and Raman analyses were performed (Fig. 2b and c). As observed from the blue lines of Fig. 2b and c, LiSEt fully dissolves in THF solvent without any side reactions, proving the high stability of LiSEt as an additive to the solvent molecules. After the addition of $P_2S_5$ in the solution, LiSEt loses its characteristic peaks and small unknown peaks are identified (red line in Fig. 2b). This result directly proves the chemical reaction between $P_2S_5$ and LiSEt, which is further supported by the Raman analysis (Fig. 2c). Any signal related to $P_2S_5$ is not detected in the mixture of $P_2S_5$ and LiSEt (red line in Fig. 2c), indicating that the bond breaking of $P_2S_5$ is promoted by the LiSEt nucleophile. The disappearance of $P_2S_5$ signals after the formation of soluble composites is well matched to a previous report.[23] In this respect, it is identified that the strong nucleophile (*i.e.*, LiSEt) can break the P–S bond of $P_2S_5$, which results in the formation of soluble intermediates in THF solvent.

Considering the results of the solubility test and bonding analyses above, we schematically describe the possible processes for the formation of the $Li_3PS_4$ SE (Fig. 3). Two moles of LiSEt are required to react with one mole of $P_4S_{10}$ because the solution becomes fully transparent at a 1 : 1 molar ratio of $P_2S_5$ and LiSEt. In the transparent solution with $LiSEt \cdot P_2S_5$, we
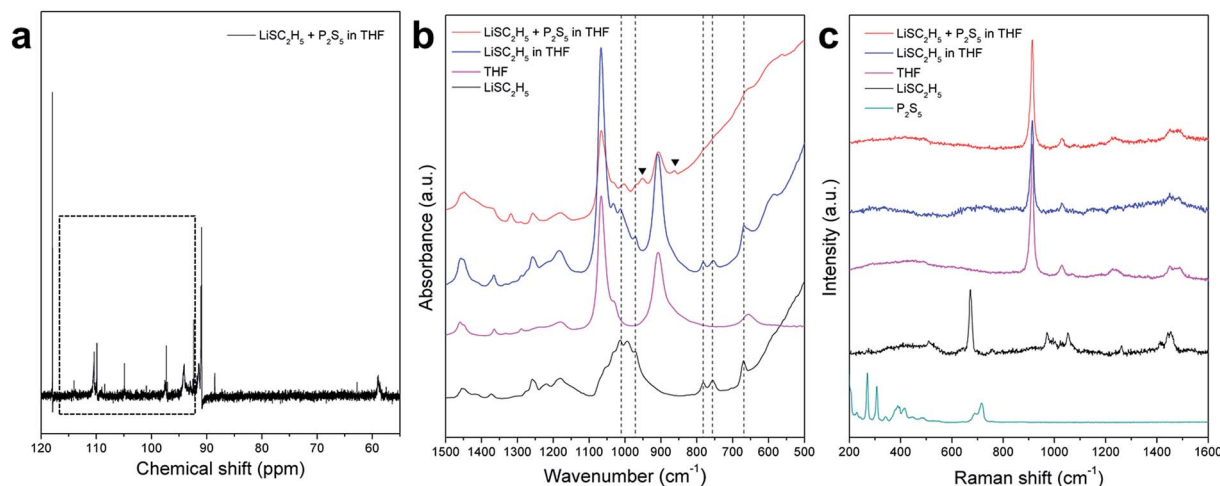


Fig. 2 (a) P-NMR, (b) FT-IR, and (c) Raman analyses of the THF solutions dissolving $P_2S_5$ and $LiSC_2H_5$ at a 1 : 1 molar ratio.
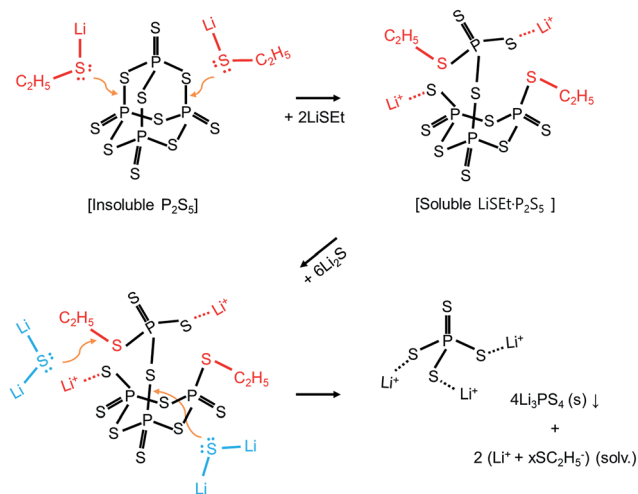
Fig. 3   Schematic illustration of the processes for the formation of the $Li_3PS_4$ solid electrolyte promoted by a nucleophile of $LiSC_2H_5$.



Fig. 4   (a and b) SEM images, (c) EDS elemental mapping result, and (d) EDS elemental analysis of the synthesized $LiSEt@Li_3PS_4$ solid electrolyte.

added $Li_2S$ to investigate whether conductive β-$Li_3PS_4$ is formed. We expected a chemical reaction between $LiSEt·P_2S_5$ and $Li_2S$ because once P–S bonds in $P_2S_5$ are opened, the asymmetric structure of the complex can easily engage in successive reactions. The precipitation of white powders was observed after the addition of $Li_2S$ into the $LiSEt·P_2S_5$ solution, and we determined that the precipitate ($LiSEt@Li_3PS_4$) is composed of β-$Li_3PS_4$, as discussed later.

By following this synthesis process, reaction kinetics can be improved because the $LiSEt·P_2S_5$ (solv.) complex has greatly enhanced the chances of reacting with $Li_2S$ (s) in the solution while conventional solution-based synthesis methods utilized two insoluble $P_2S_5$ (s) and $Li_2S$ (s) particles. In addition, the asymmetrically opened $P_2S_5$ will have a lower activation barrier to react with $Li_2S$ compared to the pristine $P_2S_5$. Even if there are un-reacted residuals (e.g., $SC_2H_5^{-}$ or $P_xS_y·C_2H_5$), they can be easily removed during filtration and are distinguishable from the precipitates. This method provides an easy way to produce a high purity solid electrolyte, which is challenging to achieve by following conventional solution-based synthesis methods.

Scanning electron microscopy (SEM) images of the precipitated particles after heat treatment from the reaction between $LiSEt·P_2S_5$ and $Li_2S$ are shown in Fig. 4. The solution was centrifuged and filtered to collect the precipitates, which were further heat treated to remove the residual solvent. Most of the particles show a consistent cylinder-like shape (Fig. 4a and b). While the overall shape of the particle looks similar to that of a previous report using a THF solvent,[11] the average particle size is smaller and the aspect ratio is higher. This is because the different solvent–reactant interactions can affect the particle shape and size.[10,12,13]

Elemental composition of the resultant product (denoted as $LiSEt@Li_3PS_4$) was analyzed using EDS analyses as shown in Fig. 4c, d and S3.† $LiSEt@Li_3PS_4$ is composed of a sulfur and phosphor mixture, which is homogeneously detected in most of the precipitated particles. Additional SEM images at low magnification are provided in the ESI (Fig. S4†). The high
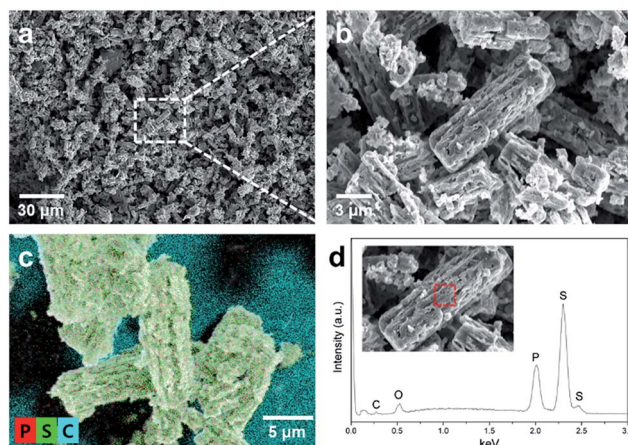
homogeneity of the final products can be attributed to the use of the liquid-phase mobile reactant (i.e., $LiSEt·P_2S_5$). Moreover, it should be noted that carbon and oxygen elements are negligible in the particles. This proves that LiSEt does not remain in the particle after the reaction, and any residuals related to LiSEt are clearly filtered out.

To investigate the properties of the $LiSEt@Li_3PS_4$ SE, Raman and X-ray diffraction (XRD) measurements were taken as shown in Fig. 5a and b, respectively. In the Raman analyses (Fig. 5a), the dominant peak around 420 cm$^{-1}$ is observed in the $LiSEt@Li_3PS_4$ (red line, after heat treatment), and its peak position is identical to the reference β-$Li_3PS_4$ demonstrating the formation of tetrahedral units of $PS_4^{3-}$.[11,12,27] Therefore, it is concluded that the final product is mostly composed of conductive β-$Li_3PS_4$. The same characteristic peak is also observed in the sample before the heat treatment, which
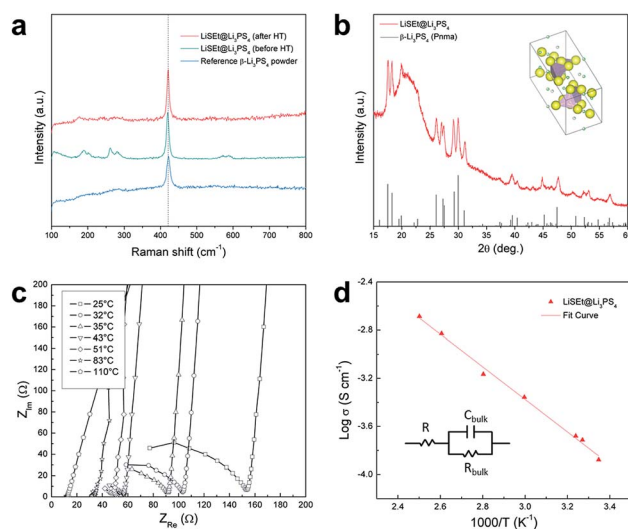


Fig. 5   (a) Raman and (b) XRD spectra of the synthesized $LiSEt@Li_3PS_4$ solid electrolyte. (c) Nyquist plots and (d) Arrhenius plots of the $LiSEt@Li_3PS_4$ solid electrolyte at different temperatures using a blocking electrode cell (inset: equivalent circuit model).

7372 | J. Mater. Chem. A, 2018, 6, 7370–7374

This journal is © The Royal Society of Chemistry 2018

implies that the LiSEt·$P_2S_5$ chemically reacted with $Li_2S$ and formed the tetrahedral units of $PS_4^{3-}$ in THF solvent. Peaks around 200–300 cm$^{-1}$ are attributed to solvent molecules bonded to lithium ions, which decreased after heat treatment in accordance with a previous report.[11] It is worth noting that any signal related to LiSEt was not detected, which corresponds well with the results of EDS analysis (Fig. 4d), supporting that LiSEt was fully removed.

The structural properties of LiSEt@$Li_3PS_4$ are analyzed as shown in Fig. 5b. All the peaks matched well with β-$Li_3PS_4$ (*Pnma* space group) without any by-product. Also, the crystallinity of LiSEt@$Li_3PS_4$ is higher than that of the reference $Li_3PS_4$ SE prepared without the addition of LiSEt (Fig. S5†). Considering impurities can precipitate in grain boundaries and greatly decrease conductivity,[12,16] making a soluble intermediate and producing high purity SEs will be essential for synthesizing high quality LPS SEs. To measure the conductivity of LiSEt@$Li_3PS_4$, electrochemical impedance spectroscopy (EIS) was analyzed using a blocking electrode cell as shown in Fig. 5c and d. LiSEt@$Li_3PS_4$ shows a high conductivity of $1.32 \times 10^{-4}$ S cm$^{-1}$ at room temperature (RT) and $1.48 \times 10^{-3}$ S cm$^{-1}$ at 110 °C with an activation energy ($E_a$) of 25.93 kJ mol$^{-1}$. This value is comparable to one of the highest recorded conductivities achieved by the nanoporous $Li_3PS_4$ SE ($1.64 \times 10^{-4}$ S cm$^{-1}$ at RT) synthesized by using the solution-based method,[11] and slightly higher than that of a commercial β-$Li_3PS_4$ powder (Fig. S6†). The high conductivity of LiSEt@$Li_3PS_4$ is expected considering that the soluble intermediate helps to enhance particle homogeneity and prevent the co-precipitation of residuals resulting in the formation of the purified β-$Li_3PS_4$ SE. Additionally, the electrochemical performance of the LiSEt@$Li_3PS_4$ solid electrolyte is evaluated by cyclic voltammetry and galvanostatic cycling tests (Fig. S7†). A stable electrochemical window of −0.5 to 6 V is observed in cyclic voltammetry and a stable cycling of the lithium metal is demonstrated during cycling tests.

## Conclusions

We developed a solution-based method to synthesize an $Li_2S$–$P_2S_5$ solid electrolyte by adding a nucleophilic agent of LiSEt (*i.e.*, $LiSC_2H_5$). We demonstrated that the nucleophile can react with $P_2S_5$, forming soluble intermediates (LiSEt·$P_2S_5$) in THF solvent. The intermediates can further react with $Li_2S$, resulting in the formation of β-$Li_3PS_4$. By tuning the reaction protocol, a kinetically and thermodynamically favorable reaction (the reaction between LiSEt·$P_2S_5$ (solv.) and $Li_2S$ (s)) can be realized, which is difficult to achieve using conventional solid-to-solid reactions. Because residuals or additives of LiSEt can be readily removed during filtration, a high purity β-$Li_3PS_4$ solid electrolyte can be produced with a high conductivity ($1.32 \times 10^{-4}$ S cm$^{-1}$ at RT). This approach will provide insights into investigating new synthesis methods for high quality solid electrolytes.

## Conflicts of interest

There are no conflicts to declare.

## Acknowledgements

## References

1 N. Kamaya, K. Homma, Y. Yamakawa, M. Hirayama, R. Kanno, M. Yonemura, T. Kamiyama, Y. Kato, S. Hama, K. Kawamoto and A. Mitsui, *Nat. Mater.*, 2011, **10**, 682–686.

2 Y. Wang, W. D. Richards, S. P. Ong, L. J. Miara, J. C. Kim, Y. Mo and G. Ceder, *Nat. Mater.*, 2015, **14**, 1026–1031.

3 A. Manthiram, X. Yu and S. Wang, *Nat. Rev. Mater.*, 2017, **2**, 16103.

4 Y. Kato, S. Hori, T. Saito, K. Suzuki, M. Hirayama, A. Mitsui, M. Yonemura, H. Iba and R. Kanno, *Nat. Energy*, 2016, **1**, 16030.

5 Y. Seino, T. Ota, K. Takada, A. Hayashi and M. Tatsumisago, *Energy Environ. Sci.*, 2014, **7**, 627–631.

6 F. Mizuno, A. Hayashi, K. Tadanaga and M. Tatsumisago, *Adv. Mater.*, 2005, **17**, 918–921.

7 A. Hayashi, S. Hama, F. Mizuno, K. Tadanaga, T. Minami and M. Tatsumisago, *Solid State Ionics*, 2004, **175**, 683–686.

8 A. Hayashi, S. Hama, H. Morimoto, M. Tatsumisago and T. Minami, *J. Am. Chem. Soc.*, 2001, **84**, 477–479.

9 F. Mizuno, A. Hayashi, K. Tadanaga and M. Tatsumisago, *Electrochem. Solid-State Lett.*, 2005, **8**, A603–A606.

10 M. Calpa, N. C. Rosero-Navarro, A. Miura and K. Tadanaga, *RSC Adv.*, 2017, **7**, 46499–46504.

11 Z. Liu, W. Fu, E. A. Payzant, X. Yu, Z. Wu, N. J. Dudney, J. Kiggans, K. Hong, A. J. Rondinone and C. Liang, *J. Am. Chem. Soc.*, 2013, **135**, 975–978.

12 R. C. Xu, X. H. Xia, Z. J. Yao, X. L. Wang, C. D. Gu and J. P. Tu, *Electrochim. Acta*, 2016, **219**, 235–240.

13 H. Wang, Z. D. Hood, Y. Xia and C. Liang, *J. Mater. Chem. A*, 2016, **4**, 8091–8096.

14 M. Calpa, N. C. Rosero-Navarro, A. Miura and K. Tadanaga, *Inorg. Chem. Front.*, 2018, **5**, 501–508.

15 N. H. H. Phuc, K. Morikawa, M. Totani, H. Muto and A. Matsuda, *Solid State Ionics*, 2016, **285**, 2–5.

16 S. Ito, M. Nakakita, Y. Aihara, T. Uehara and N. Machida, *J. Power Sources*, 2014, **271**, 342–345.

17 S. Teragawa, K. Aso, K. Tadanaga, A. Hayashi and M. Tatsumisago, *J. Power Sources*, 2014, **248**, 939–942.

18 S. Teragawa, K. Aso, K. Tadanaga, A. Hayashi and M. Tatsumisago, *Chem. Lett.*, 2013, **42**, 1435–1437.

19 S. Teragawa, K. Aso, K. Tadanaga, A. Hayashi and M. Tatsumisago, *J. Mater. Chem. A*, 2014, **2**, 5095–5099.

20 Y. Wang, Z. Liu, X. Zhu, Y. Tang and F. Huang, *J. Power Sources*, 2013, **224**, 225–229.

21 D. C. Gerbino, D. Augner, N. Slavov and H.-G. Schmalz, *Org. Lett.*, 2012, **14**, 2338–2341.

This journal is © The Royal Society of Chemistry 2018

*J. Mater. Chem. A*, 2018, **6**, 7370–7374 | 7373

22 J. Cvengroš, S. Neufeind, A. Becker and H.-G. Schmalz, *Synlett*, 2008, **2008**, 1993–1998.

23 Q. Pang, X. Liang, A. Shyamsunder and L. F. Nazar, *Joule*, 2017, **1**, 871–886.

24 M. Gobet, S. Greenbaum, G. Sahu and C. Liang, *Chem. Mater.*, 2014, **26**, 3558–3564.

25 H. Eckert, Z. Zhang and J. Kennedy, *Chem. Mater.*, 1990, **2**, 273–279.

26 C. Jameson and J. Mason, *Multinuclear NMR*, Plenum Press, 1987.

27 Z. Lin, Z. Liu, W. Fu, N. J. Dudney and C. Liang, *Angew. Chem.*, 2013, **125**, 7608–7611.